



Modelling and identification of delamination in double-layer beams by the virtual distortion method

Anita Orłowska, Przemysław Kołakowski*, Jan Holnicki-Szulc

Smart-Tech Centre, Institute of Fundamental Technological Research, Świętokrzyska 21, 00-049 Warsaw, Poland¹

ARTICLE INFO

Article history:

Received 1 August 2007

Accepted 23 May 2008

Available online 30 July 2008

Keywords:

Delamination
Double-layer beams
Identification
Inverse problem

ABSTRACT

The problem of modelling and identification of delamination in double-layer beams has been undertaken within the framework of the virtual distortion method. For delamination modelling, a concept of the contact layer has been proposed, assuming simple but effective truss connections. The laminate layers have been modelled with Bernoulli beams. Good correspondence of the delamination model with experiments has been observed despite disregarding the friction between layers. An algorithm for off-line identification of delamination, solving an inverse problem with the use of gradient optimization, has been proposed. For double cantilever beam examples, two co-existing delamination zones have been successfully detected. An idea of on-line identification of delamination has been put forward, too.

© 2008 Elsevier Ltd. All rights reserved.

1. Introduction

1.1. Overview of recent papers on delamination

Fast development of composites has provided the incentive for dealing with one of the most severe defects in such structures – delamination. A review of methods dealing with delamination in the 1990s is provided by Zou et al. [1].

Many recent papers devoted to delamination are focused on the problem of proper modelling of delamination initiation and growth. Meo and Thieulot [2] compare four different ways of modelling delamination growth, i.e. cohesive zone, non-linear springs, birth and death elements and tiebreak contact, applied to a double cantilever beam test. Only the tiebreak contact method failed to match experimental results due to the adopted stress-based failure criterion. Iannucci [3] proposes an interface modelling technique for explicit FE codes. In the technique, based on fracture mechanics, not only a stress threshold for damage commencement, but also critical energy release rate for particular delamination mode is used. The interface modelling technique was applied to a series of common delamination tests, including an experimentally validated impact test, to show the superiority of the approach over standard stress-based failure criterion. Conventional interface modelling methods suffer from several shortcomings i.e. interface elements have to be introduced *a priori*, spurious deformation occurs at onset of delamination, traction oscillations accompany the process of delamination growth, finite elements have to be aligned

with potential delamination surface. These unwanted features can be avoided by modelling delamination at a mesoscopic level, proposed by De Borst and Remmers [4], who use the partition-of-unity property of the finite element shape functions. The strength of the approach is emphasized by the possibility of its consistent extension to large strains.

Next important problem undertaken by researchers is the search for such dynamic responses of the delaminated structure, which are sensitive to detecting damage. Kim and Hwang [5] examine the influence of debonding in face layers of honeycomb sandwich beams on frequency response functions (FRF). By extracting natural frequencies and damping ratios from the FRFs and using modal parameter identification, the extent of delamination can be reliably determined. Li et al. [6] describe the potential of random decrement signatures along with neural networks in delamination detection. Due to inaccurate damping modelling, there was a mismatch between their experimental and numerical results for glass fibre reinforced beams. Zak [7] demonstrates that damped non-linear vibrations are very sensitive to delamination location and length, depending upon excitation. Single delaminations in simply-supported and cantilever beams were considered. Additional peaks in FRFs as well as changes in hysteresis loops of transverse displacements of the beams were observed due to delaminations.

Another group of papers propose solutions to the inverse problem of identification of delamination, belonging to the main stream of structural health monitoring (SHM). Bois et al. [8] inversely identify delamination by applying a piezoelectric transducer to the laminate. A model including both the delaminated zone and the piezoelectric ply was proposed. Electromechanical impedance of a transducer working both as actuator and sensor was measured.

¹ <http://smart.ippt.gov.pl/>.

* Corresponding author.

E-mail address: pkolak@ippt.gov.pl (P. Kołakowski).

An 18 cm 16-ply beam equipped with six transducers was investigated for the frequencies between 100 Hz and 30 kHz. The objective function included frequency and mode amplitude terms comparing the measured and simulated results. Single delaminations at the end of the beam and inside the beam were identified with good accuracy. Ishak et al. [9] use soft-computing methods to detect delamination via inverse analysis. First, the strip element method (SEM) was employed to train the multilayer neural network. Excitation frequencies in the range 10–30 kHz were used to identify delamination regions in a 20-ply laminated beam of just 4 cm length. Experiments were carried out using a scanning laser vibrometer to validate the proposed approach. If discrepancies between experimental and SEM results occurred, the neural network was re-trained to improve the quality of identification. The soft-computing approach proved effective in identification of single delamination for the considered range of frequencies. Schnack et al. [10] propose an iterative method of identification of single delamination by solving an inverse problem. A general ill-posed problem described by the Kohn–Vogelius functional was transformed into a coupled system of well-posed Euler–Lagrange equations and a smooth iterative numerical solution was proposed. Surface deformations of a 16-ply composite specimen were measured using laser modulation and Michelson interferometer. Delamination zones close to specimen boundaries as well as internal ones were successfully detected. Ramanujam et al. [11] apply classical optimization to identify delamination via inverse analysis. Their numerical considerations included a simply supported 4-ply laminate beam with a single embedded delamination. The beam was equipped with eight uniformly distributed sensors. Squared difference between the actual and measured (simulated by FEM) strains was considered and Nelder–Mead gradient-free optimization method was employed to find a solution to the inverse problem. Many starting points were required to obtain a minimum. Generally, only the sensors close to delamination showed a deviation from the reference response. The quality of identification results was improved by considering a deflection term in the objective function and multiple loading conditions. The approach was presented for detection of a single, 2-dimensional, through-delamination, solely by numerical simulation.

1.2. Objectives of the paper

This paper takes up two important problems regarding composite beams. The first one is proper modelling of delamination between the layers of laminate, the other one – effective identification of delamination zones.

For modelling of delamination, a concept of the contact layer between laminates has been proposed. The layer consists of truss elements supposed to model vanishing of the shear forces in delamination zones and providing appropriate contact conditions between the laminate layers. The two features of the contact layer, modifying its properties in selected zones, are easy to model within the framework of the virtual distortion method (VDM), which is a fast, exact reanalysis method. By generating virtual distortions (pseudo strains), the VDM is able to introduce large modifications to the structure, which simulate vanishing of the shear forces and appropriate contact conditions in delamination zones.

The problem of identification belongs to the field of SHM, which has been developed intensively in the recent years. Many of the SHM approaches use soft-computing methods, e.g. neural networks, genetic algorithms, pattern recognition, for the solution of the problem of defect identification. In this paper, an analytical formulation is proposed based on the VDM with an underlying model updating procedure. Sensitivity information is effectively used in an optimization algorithm solving the inverse problem of a *post-*

riori identification. A concept of on-line identification, not related to the VDM, is proposed, too.

2. Parameter modification by the virtual distortion method

2.1. General characteristic of VDM

The virtual distortion method (VDM) [12] belongs to fast reanalysis methods in structural mechanics. This means that an initial FEM response is necessary for introducing further modifications by determining proper fields of virtual distortions. A comparative review of reanalysis methods can be found in [13], where equivalence between the VDM and Sherman–Morrison–Woodbury formulas is proved.

The VDM is conceptually similar to the initial strains approach. Introduction of initial strains in structures was primarily proposed to model plasticity. However, the local imposition of an initial strain leads to violation of equilibrium conditions and the solution proceeds in iterations. On the contrary, the VDM approach is able to produce such solution in one step thanks to defining all local–global interrelations in a structure in advance. The collection of all the local–global responses, including information about structural topology, materials and boundary conditions, is called the influence matrix within the framework of VDM. This matrix makes an essential difference between the VDM and initial strains approach.

The VDM has been used in various problems of structural design (e.g. prestress), optimization (e.g. topology remodelling) and control (e.g. damping of vibrations) thus far. Some of its applications have been recently described in [14]. As presented in this paper, it has also turned out to be a promising tool for identification in SHM.

2.2. Influence matrix

In further description let us assume that the lowercase indices refer to elements and the uppercase ones to nodes. Einstein's summation convention is used. Underlined indices are exempt from summation. Let us first demonstrate the concept of the influence matrix for truss structures in static analysis.

Each component of the influence matrix D_{ij} describes strains in the truss member i caused by the unit *virtual distortion* $\varepsilon_j^0 = 1$ applied to the member j . For truss structures, the unit virtual distortion is simply a unit axial tensile strain. The unit virtual distortion is imposed in numerical calculations as a pair of *self-equilibrated compensative forces* of reverse signs, equivalent to a unit strain, applied to the nodes of the strained element. The influence matrix D_{ij} collects n influence vectors, where n denotes the number of truss elements. In order to build an influence vector, a solution of a standard linear elastic problem by the FEM has to be found:

$$K_{MN}u_N = f_M \quad (1)$$

with K being the stiffness matrix. Usually, the obtained global displacements serve to calculate a corresponding response in local strains:

$$\varepsilon_i = G_{iN}u_N \quad (2)$$

with G being the geometric matrix, which transforms global degrees of freedom to local strains. The response in strains is most often considered for building an influence vector. However, storage of any other required response, i.e., displacements, stresses or forces, is also useful.

The external force vector f in (1) corresponds to two compensative axial forces applied to a structural member, equivalent with application of a unit strain to the unconstrained member. The compensative forces are applied to the diagonal element, taken out of

the structure, shown in Fig. 1. The response of the structure to the imposition of the unit virtual distortion $\varepsilon_5^0 = 1$ is depicted by the deformed configuration in Fig. 1. Thus to build the influence matrix D_{ij} , n solutions of a linear elastic problem have to be found. The set (1) has to be solved with n different right-hand sides corresponding to n pairs of compensative forces applied successively in each structural member. This way, the influence matrix stores information about the entire structure properties including topology, material characteristics and boundary. Note that the static influence matrix for statically determinate structures becomes identity. This is due to the fact the such structures have no redundancy, i.e. no internal constraints, so the application of an initial strain to a member will not affect its neighbourhood. Thus in statics, for structures of no redundancy, the VDM loses its major numerical tool.

Analogously, the influence matrix can be built in dynamic analysis, where the response due to impact load in the first time step is looked for. Integration of the equations of motion is performed by the Newmark algorithm over some predefined period of time. In order to build the influence matrix in dynamics, a pair of self-equilibrated forces equivalent to unit strain is applied to a truss member in the first time step only. Such a perturbation introduced to the structure is called an impulse virtual distortion. In subsequent time steps, the influence of the distortion on the structure is examined over the discretized time period. Structural response in each time step corresponds to an influence vector in statics, so the collection of such responses from all time steps provides an influence “vector” in dynamics. This “vector” has an extra dimension, which is time. An assembly of dynamic influence “vectors” constitutes the dynamic influence “matrix”, which has two dimensions corresponding to the number of structural members, like in statics, and the third dimension – time. Generally, the dynamic influence matrix is time dependent, however for harmonic excitation, it becomes quasi static (2D), because only amplitudes of responses are stored.

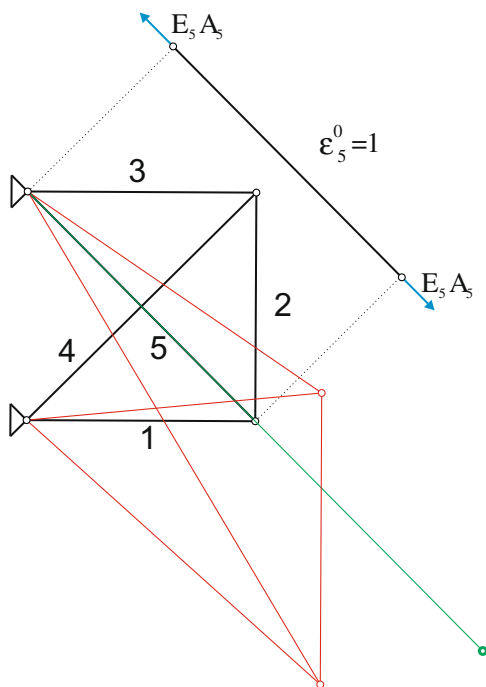


Fig. 1. Virtual distortion applied in a chosen element.

2.3. Stiffness modelling in truss elements

Let us confine our considerations to truss structures in the elastic range and analyze introducing a field of initial strains ε^0 , called *virtual distortions*, into a truss structure. This action will induce residual strains in the structure, expressed as follows (cf. [12]):

$$\varepsilon_i^R = D_{ij}\varepsilon_j^0. \tag{3}$$

Residual stresses are expressed by:

$$\sigma_i^R = E_i(D_{ij} - \delta_{ij})\varepsilon_j^0, \tag{4}$$

where E_i denotes the Young’s modulus and δ_{ij} – the Kronecker’s delta.

Assume that application of external load to the structure provokes linear elastic response ε_i^L , σ_i^L , which will be superposed with the residual response ε_i^R , σ_i^R . Thus in view of (3) and (4), we get:

$$\varepsilon_i = \varepsilon_i^L + \varepsilon_i^R, \tag{5}$$

$$\sigma_i = \sigma_i^L + \sigma_i^R = E_i(\varepsilon_i - \varepsilon_i^0). \tag{6}$$

Relation between element forces p and stresses σ is known via the cross-sectional areas A :

$$p_i = A_i\sigma_i. \tag{7}$$

Let us now take into account structural geometry modifications exemplified by changes of cross-sectional area of a member. This means considering of a modified value \hat{A} . In view of (6) and (7), we can express element forces in the *original structure* with introduced virtual distortion field, called the *distorted structure*, and in the *modified structure*, as follows:

$$p_i = E_iA_i(\varepsilon_i - \varepsilon_i^0), \tag{8}$$

$$\hat{p}_i = E_i\hat{A}_i\hat{\varepsilon}_i. \tag{9}$$

The main postulate of the VDM in static remodelling requires that local strains, including plastic ones, and forces in the distorted and modified structure are equal:

$$\varepsilon_i = \hat{\varepsilon}_i, \tag{10}$$

$$p_i = \hat{p}_i. \tag{11}$$

This postulate leads to the following relation:

$$E_iA_i(\varepsilon_i - \varepsilon_i^0) = E_i\hat{A}_i\hat{\varepsilon}_i. \tag{12}$$

Eq. (12) provides the coefficient of the stiffness change μ for each truss element i as the ratio of the modified parameter \hat{A} to the initial one A :

$$\mu_i = \frac{\hat{A}_i}{A_i} = \frac{\varepsilon_i - \varepsilon_i^0}{\varepsilon_i}. \tag{13}$$

Note that the coefficient μ_i may be equivalently expressed as the ratio of the initial to modified Young’s modulus of a truss element. If $\mu_i = 1$ we deal with an intact structure. Variation of the coefficient in the range $0 \leq \mu_i \leq 1$ means degradation of stiffness and in the range $\mu_i \geq 1$ increase of stiffness. Substituting (3) and (5) into (13) we get a set of equations for ε_j^0 , which must be solved for an arbitrary number of modified elements (usually small compared to all elements in the structure), described by the coefficient μ_i different than 1:

$$[\delta_{ij} - (1 - \mu_i)D_{ij}]\varepsilon_j^0 = (1 - \mu_i)\varepsilon_i^L. \tag{14}$$

In dynamics, a residual response is a discrete convolution of the influence matrix and virtual distortions. The time-dependent residual displacement, strain and stress vectors can be expressed as follows (cf. (3) and (4)):

$$\varepsilon_i^R(t) = \sum_{\tau=0}^t D_{ij}(t-\tau) \varepsilon_j^0(\tau), \quad (15)$$

$$\sigma_i^R(t) = E_i \left[\sum_{\tau=0}^{t-1} D_{ij}(t-\tau) + D_{ij}(0) - \delta_{ij} \right] \varepsilon_j^0(\tau). \quad (16)$$

Integration of equations of motion in time is handled by the Newmark algorithm. The previously-given relations (5)–(13) are valid for dynamics as well. While most quantities vary in time, the stiffness change coefficient, defined analogously to (13), remains time independent:

$$\mu_i = \frac{\widehat{A}_i}{A_i} = \frac{\varepsilon_i(t) - \varepsilon_i^0(t)}{\varepsilon_i(t)}. \quad (17)$$

The set of equations to be solved for distortions in dynamics looks analogously to (14):

$$[\delta_{ij} - (1 - \mu_i)D_{ij}(0)] \varepsilon_j^0(t) = (1 - \mu_i) \varepsilon_i^{\neq t}(t). \quad (18)$$

where $\varepsilon_i^{\neq t}(t)$ denotes strains cumulated before the current step t :

$$\varepsilon_i^{\neq t}(t) = \varepsilon_i^1(t) + \sum_{\tau=0}^{t-1} D_{ij}(t-\tau) \varepsilon_j^0(\tau). \quad (19)$$

Similarly to (14), the set (18) may be local if structural remodelling is performed. In identification problems however, in which the location of a damaged/degraded member is sought, the set (18) concerns all elements potentially changed – usually the whole structure.

3. Modelling of delamination

3.1. Interconnection between laminates (contact layer)

Delamination of a double-layer beam is understood in the paper as an existing defect of certain extension in the structure. The process of crack growth, leading to the existence of the defect, is not the subject of interest here. The authors have proposed the simplest possible model of delamination, taking into account the contact between the laminate layers.

This paper puts forward a proposition of introducing a special interconnection between the layers of the laminate for modelling delamination in two aspects. The principal one is that the shear

forces in the interconnection, joining two laminate layers, should vanish in delamination zones. The secondary aspect, rarely taken into account in delamination modelling, is that proper contact between laminates should exist in delamination zones. This section will be focused on explanation of how the interconnection between the laminate layers is constructed and how the VDM can be used to model its behaviour.

When modelling delamination in multi-layer composites, Timoshenko beam is appropriate to account for interactions of laminates (cf. [15]). In this paper however, the Bernoulli beam is the subject of consideration for two reasons – (i) 2D beams consisting of only two layers are considered, (ii) simplified Bernoulli model enables to perform identification of delamination by solving an inverse problem at an affordable numerical cost. In the FEM model, standard 2-noded beam elements are used for the laminate layers. The two-layer beam with the interconnection for modelling delamination is shown in Fig. 2. Middle axes of the beams are depicted with continuous horizontal white lines in Fig. 2a. In between, the interconnection of the laminates, consisting of the diagonal and vertical truss elements joining the middle axes of the beams, is introduced. The role of the diagonal truss elements is to simulate vanishing of shear forces in delamination zones. The role of the vertical truss elements is to ensure proper contact conditions between the laminates. Stiffness characteristic of the vertical truss elements, shown in Fig. 3, is assumed in an arbitrary way, enabling some penetration of one laminate layer into another. In fact this is not the case in reality, however this adjustment of stiffness of the vertical elements turned out to be very important when matching the numerical model to experiments. Friction is not taken into account in this paper, although there is no formal obstacle to include it within the framework of VDM. The reason is again to minimize numerical effort.

3.2. Modelling of delamination by VDM

The contact layer has a modular structure. Each section of the layer consists of three elements – two diagonals denoted by A and B and one vertical denoted by C in Fig. 4.

If delamination is to be modelled in selected sections of the contact layer, then the following conditions in the diagonal elements A, B have to be fulfilled:

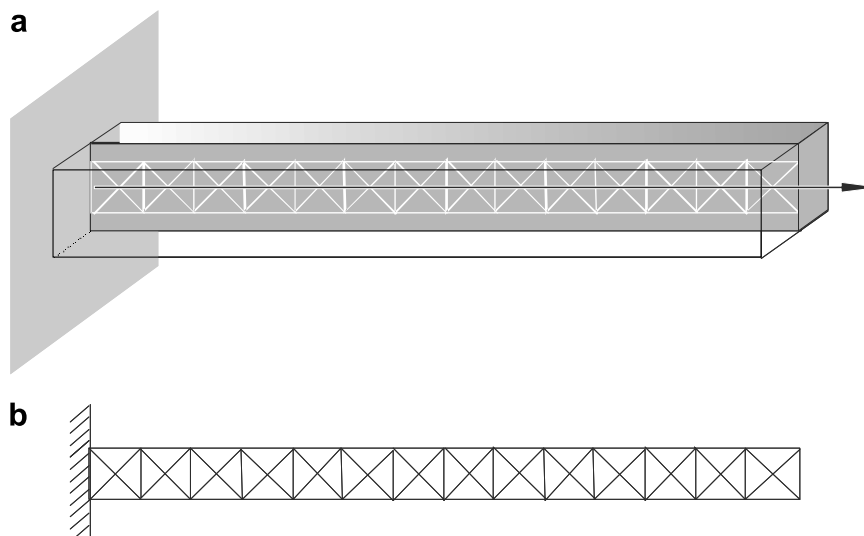


Fig. 2. (a) Double cantilever beam with the contact layer supposed to model delamination; (b) contact layer to be analysed by VDM.

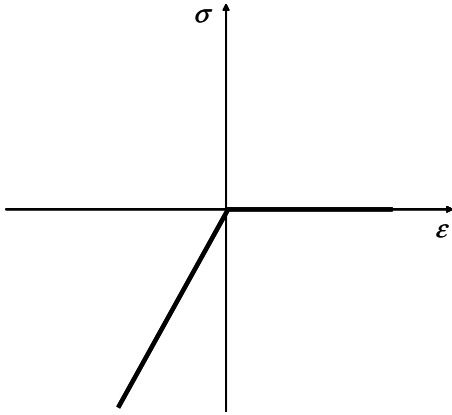


Fig. 3. Stress–strain relationship for the vertical elements of the contact layer.

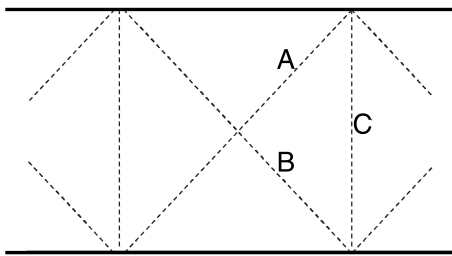


Fig. 4. Zoomed section of the contact layer.

$$\mu_i^A = 0 \Rightarrow \varepsilon_i^{0A} = \varepsilon_i^A, \tag{20}$$

$$\mu_i^B = 0 \Rightarrow \varepsilon_i^{0B} = \varepsilon_i^B. \tag{21}$$

The superscripts A, B at a quantity refer to corresponding diagonal elements. Depending upon the kind and direction of load applied to the structure, the two laminates will either be in contact or not. This is accounted for by examining the sign of strain in the vertical element C. If tensile strain is encountered in the vertical elements, then appropriate distortions are generated, modelling no contact between the laminate layers:

$$\mu_i^C = 0 \Rightarrow \varepsilon_i^{0C} = \varepsilon_i^C \quad \text{if } \varepsilon_i^C > 0. \tag{22}$$

If compressive strain is encountered in the vertical elements, then no distortions are generated and the layers stay in full contact in spite of local delamination in between:

$$\mu_i^C = 1 \Rightarrow \varepsilon_i^{0C} = 0 \quad \text{if } \varepsilon_i^C \leq 0. \tag{23}$$

One should remember that the assumed characteristic (see Fig. 3) allows for some penetration of one layer into another, which gives the possibility of tuning the numerical model to experiment.

Implications of the conditions (20) and (21) say that distortions are equal to total strains, however these relations cannot be directly used because total strains are *a priori* unknown. In order to determine distortions one has to solve the general system of Eq. (14), which allows for an arbitrary change of the coefficient μ :

$$\begin{bmatrix} \delta_{ij} - (1 - \mu_i^A)D_{ij}^A & -(1 - \mu_i^B)D_{ij}^B \\ -(1 - \mu_i^A)D_{ij}^A & \delta_{ij} - (1 - \mu_i^B)D_{ij}^B \end{bmatrix} \begin{bmatrix} \varepsilon_j^{0A} \\ \varepsilon_j^{0B} \end{bmatrix} = \begin{bmatrix} (1 - \mu_i^A)\varepsilon_i^{LA} \\ (1 - \mu_i^B)\varepsilon_i^{LB} \end{bmatrix}. \tag{24}$$

Simultaneously, the conditions $\mu = 0$ (cf. (20) and (21)) must be substituted into the system to model delamination in the required zone. The distortion vector and influence matrix have been divided into parts corresponding to elements A and B, which facilitates the organization of the algorithm and code. As soon as distortions in

diagonal elements are generated, it is necessary to check the sign of strain in vertical elements, using a prediction, which is supposed to reflect its sign (not the value) correctly (see section 3.3 for comments):

$$\varepsilon_i^C = \varepsilon_i^{LC} + D_{ij}^A \varepsilon_j^{0A} + D_{ij}^B \varepsilon_j^{0B}. \tag{25}$$

If it turns out that tensile stress is present, then the system of Eq. (24) has to be extended, to include the calculation of distortion in vertical elements, too:

$$\begin{bmatrix} \delta_{ij} - (1 - \mu_i^A)D_{ij}^A & -(1 - \mu_i^B)D_{ij}^B & -(1 - \mu_i^C)D_{ij}^C \\ -(1 - \mu_i^A)D_{ij}^A & \delta_{ij} - (1 - \mu_i^B)D_{ij}^B & -(1 - \mu_i^C)D_{ij}^C \\ -(1 - \mu_i^A)D_{ij}^A & -(1 - \mu_i^B)D_{ij}^B & \delta_{ij} - (1 - \mu_i^C)D_{ij}^C \end{bmatrix} \begin{bmatrix} \varepsilon_j^{0A} \\ \varepsilon_j^{0B} \\ \varepsilon_j^{0C} \end{bmatrix} = \begin{bmatrix} (1 - \mu_i^A)\varepsilon_i^{LA} \\ (1 - \mu_i^B)\varepsilon_i^{LB} \\ (1 - \mu_i^C)\varepsilon_i^{LC} \end{bmatrix} \tag{26}$$

Thus, the algorithm of delamination modelling consists of the following stages:

1. Initialize – influence matrix, linear response.
2. Solve the set (24) to determine distortions for vanishing of shear forces in the contact layer.
3. Check the sign of strain in vertical elements of the contact layer using (25).
4. If no contact between laminate layers appears, solve extended set (26) to determine distortions.
5. Update strains in the whole structure.

In dynamics, the algorithm repeats the same stages in every time step processed by the Newmark integration procedure. All quantities, except for the modification coefficient μ , are then time dependent. Computations are costlier compared to statics, because the amount of data is multiplied by the number of time steps.

3.3. Numerical example in statics

A double cantilever beam, shown in Fig. 5, of 1 m length and 0.02 m height, has been chosen to demonstrate the modelling of delamination by VDM in statics. The contact layer is divided into 10 sections with three elements of type A, B, C in each one, resulting in 30 connecting elements altogether. The assumed geometrical and material data are listed in Table 1.

Delamination zone extending through four sections 6–9 is analyzed (cf. Fig. 5). Two cases of static loading are considered. Calculations performed by the FEM package ANSYS serve as verification of VDM results.

The first load case, shown in Fig. 5, is a single vertical force applied to the top beam at the cantilever’s free end. The intention is to examine appropriateness of delamination modelling by VDM for the case of closed crack. Fig. 6 depicts axial strains in diagonal elements A (numbered 1–10) and B (numbered 11–20) of the contact layer for the structure with the assumed delamination. It is natural that strains in the contact layer are larger in these elements A and B, which are the closest to the delamination zone. Axial strains in vertical elements C are calculated according to (25). For the considered loading, the first term in formula (25) is negligibly small and the second and third terms cancel out due to almost identical value and reverse signs of strains in elements A, B.

The second case of loading, corresponding to the structure with open crack, is presented in Fig. 7. Axial strains in elements A and B, shown in Fig. 8, appear only within the delamination zone and are of the same sign and value. Contrary to the first loading case (cf. Fig. 5), axial strains in contact elements C, depicted in Fig. 9, are now two orders of magnitude larger than in diagonal elements A, B.

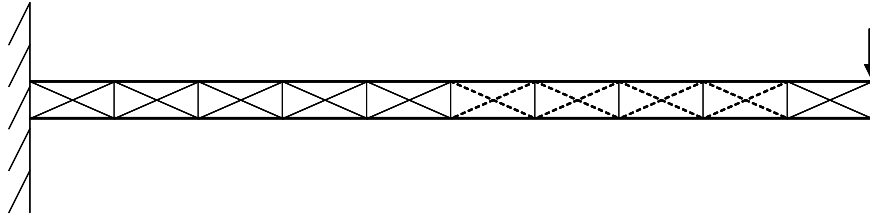


Fig. 5. Double cantilever beam subjected to 1st static loading.

Table 1
Data for the double-layer beam subjected to static test

Quantity	Beam element	Connecting truss element
Young's modulus (GPa)	70	30
Cross-section area (m ²)	5 × 10 ⁻⁵	5 × 10 ⁻⁵
Density (kg/m ³)	3300	1

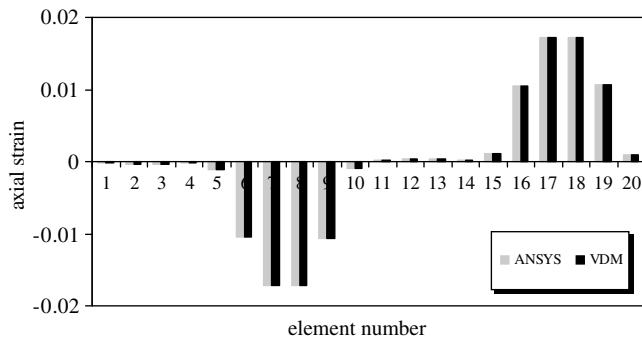


Fig. 6. Axial strains in elements A, B of the contact layer for the 1st static loading.

For calculations with ANSYS, the contact elements CONTA171 and the associated TARGE169 were used. The coefficient of normal contact stiffness factor was FKN = 0.1 and the coefficient of sliding contact stiffness factor was FKT = 1.0. Agreement of VDM results with ANSYS is very good.

3.4. Numerical example in dynamics

Another double cantilever beam of 1 m length and 0.02 m height with slightly different material data, shown in Table 2 (cf. Table 1 in section 3.3), is considered in dynamic test. Delamination zone, presented in Fig. 10, extends now through three sections 5–7. An impulse force of magnitude *P* and duration equal to one period of sine was applied within the delamination zone.

Fig. 11 shows the time history of strain in the vertical element, marked by a bold line in Fig. 10, under the applied force, for the intact and delaminated structure. The VDM results, depicted in Fig. 11, follow the ANSYS computations very closely, therefore the latter ones were not shown for the clarity of presentation. It is apparent that the strains grow considerably when the crack be-

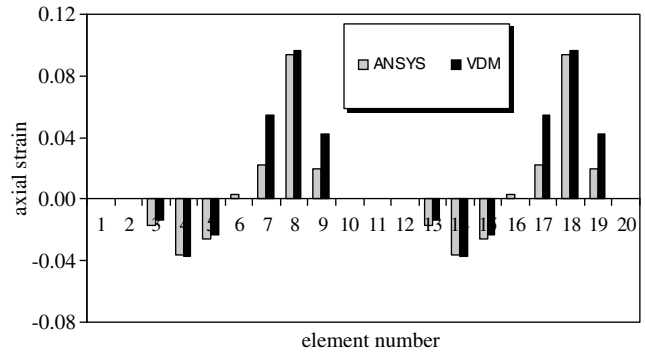


Fig. 8. Axial strains in elements A, B of the contact layer for the 2nd static loading.

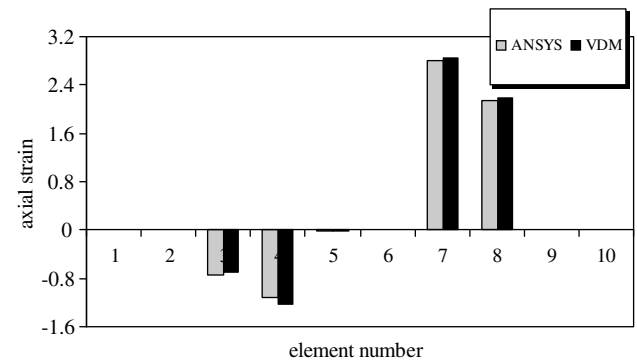


Fig. 9. Axial strains in elements C of the contact layer for the 2nd static loading.

Table 2
Data for the double-layer beam subjected to dynamic test

Quantity	Beam element	A, B element	C element
Young's modulus (GPa)	70	10	1
Cross-section area (m ²)	5 × 10 ⁻⁵	5 × 10 ⁻⁵	5 × 10 ⁻⁵
Density (kg/m ³)	3300	1	1

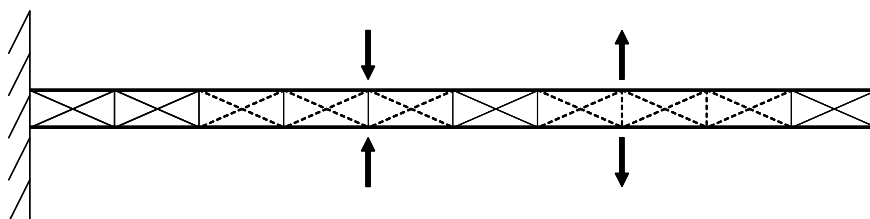


Fig. 7. Double cantilever beam subjected to 2nd static loading.

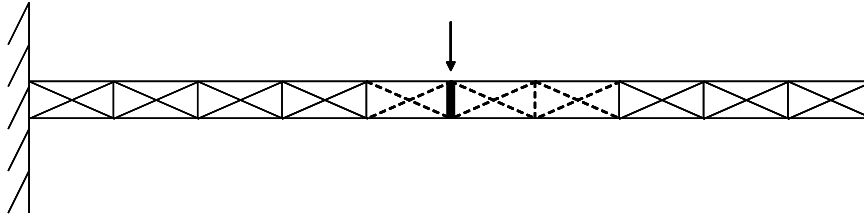


Fig. 10. Double cantilever beam subjected to dynamic loading.

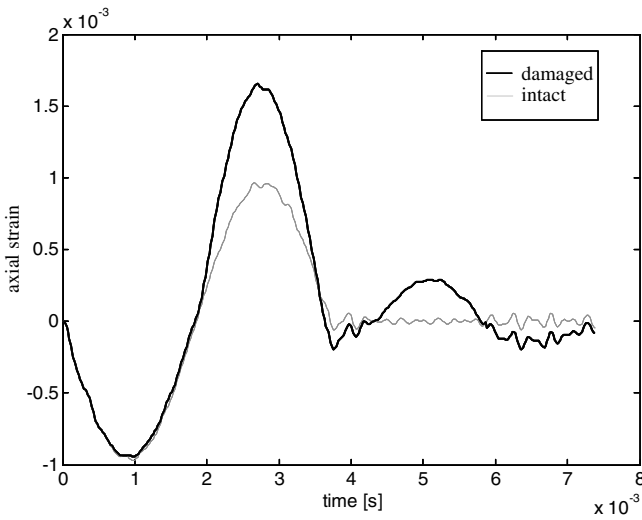


Fig. 11. Axial strains in the element C, marked bold in Fig. 10, under the applied load.

tween the upper and lower beam gets open. This can be clearly seen for the time range between 0.002 s and 0.004 s. The effect is also visualized in Fig. 12, presenting the shape of the deformed structure, working in the open crack mode at the point of maximum strain.

3.5. Experimental validation in dynamics

An experimental validation of numerical model of delamination was carried out. A double cantilever structure, schematically depicted in Fig. 13a, consisting of two aluminium beams – each one of 0.8100 m length, 0.0250 m width and 0.0024 m height – was

investigated. The two beams were joined by 10 screws (see Fig. 14a), placed in uniform distances over the length and marked by vertical lines in Fig. 13a. This division was naturally adopted in structuring the VDM-based contact layer (see Fig. 13b), whose vertical elements are placed exactly at the location of screws, resulting in 10 sections altogether. The height of the contact layer, joining middle axes of the beams, is equal to the height of one beam i.e. 0.0024 m. The contact layer consists of 20 truss elements of type A, B (diagonal) and 10 truss elements of type C (vertical). Each aluminium beam is divided into 80 finite beam elements, so there are 8 beam elements in each of the 10 sections of the contact layer.

The measuring system, presented in Fig. 15a, was used in experiment. It consisted of:

1. an activation line, including signal generator, amplifier and piezoelectric actuator (applying a bending moment to the beam), shown in Fig. 14b.
2. a detection line, including a piezoelectric sensor, depicted in Fig. 14c, conditioning amplifier and oscilloscope.

Both lines of the measuring system were coupled by a controlling computer.

A windowed sine signal, shown in Fig. 15b, was applied to the structure by the actuator. The response in terms of voltage, proportional to strains, was captured by the sensor for two cases. The first one was the intact structure with no delamination. The second one was the damaged structure with delamination extending through three sections of the contact layer. The defect was modelled by removing two screws, marked by dashed lines in Fig. 13a, from the central part of the beam.

Numerical model of the structure was created and tuned to experimental response using the intact structure configuration. The tuned data read: Young's modulus $E = 41 \text{ GPa}$ for the beam elements and stiffness $EA = 925 \times 10^3 \text{ Pa m}^2$ for the truss elements in the contact layer.

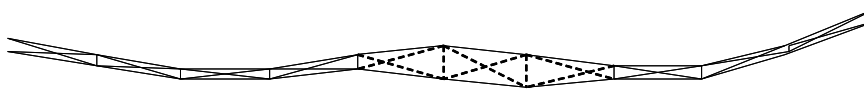


Fig. 12. Structural deflection in the open crack mode.

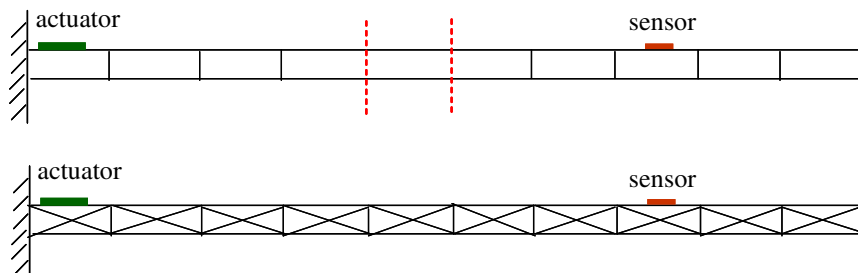


Fig. 13. (a) Layout of a double-layer cantilever beam; (b) the corresponding contact layer.

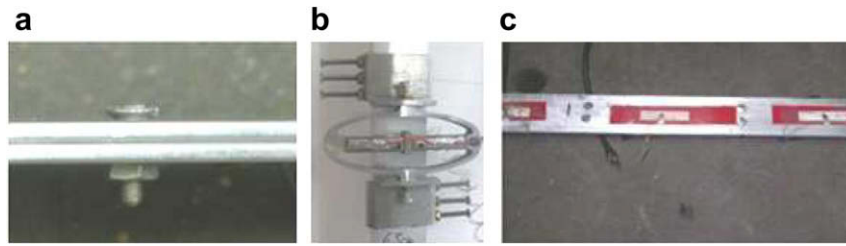


Fig. 14. (a) Screw connection; (b) actuator; (c) sensors.

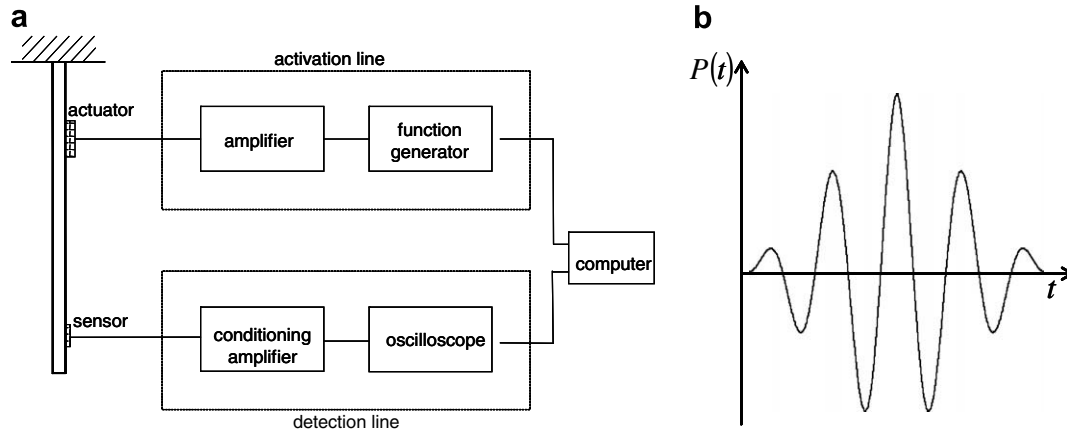


Fig. 15. (a) Measuring system; (b) excitation signal.

Arbitrary delamination was introduced to the structure in experiment by removing two screws. The excitation frequency was close to the 3rd eigenfrequency of the structure with delamination. Responses of the damaged structure were collected and compared with numerical analysis using the previously tuned model. Comparison of the first eigenfrequencies between experiment and numerical analysis is presented in Table 3. The highest discrepancy can be observed for the 4th eigenfrequency. This mode has two of its three nodal points, i.e. zero-displacement points, coinciding with the start and end of the delamination zone. Therefore the beams working in the 4th eigenmode should be influenced by contact and friction within the delamination zone more significantly than in any other mode. This seems to be the reason of the numerical–experimental discrepancy as friction has been disregarded in the numerical model.

Good agreement of results between the experiment and VDM model is shown in Fig. 16, presenting time histories for the intact and damaged structure.

4. Identification of delamination

4.1. Formulation of an off-line problem

Depending upon the application, the important problem of defect identification can be handled in an off-line (*post factum*) or on-

Table 3
Conformity of the numerical model to experiment

Eigenfrequency	Experimental	Numerical
1	5.00	5.05
2	29.70	29.36
3	70.60	73.27
4	140.00	129.05
5	199.00	199.30

line (real-time) procedure. This section is devoted to the problem of off-line identification of delamination by employing VDM-based gradient optimization. Within the framework of VDM, an analytical sensitivity analysis can be effectively performed. Therefore the inverse problem of identification can be solved using classical optimization tools i.e. gradients of the objective function with respect to a design variable.

Usually, frequencies and mode shapes obtained via modal analysis enter the objective function in the inverse problem of identification. In this article strains have been chosen for the purpose. The reason is that on the one hand strains can be easily modelled in VDM (cf. (3) and (5)), on the other - they can be measured by piezoelectric sensors. One more advantage is that the variation of strains in dynamics is relatively smooth (compared to accelera-

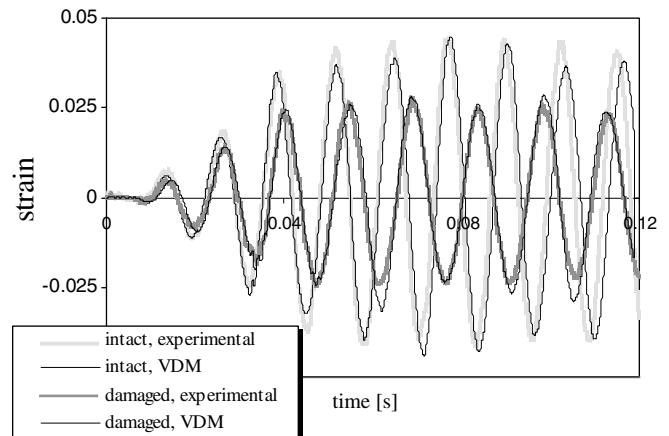


Fig. 16. Numerical vs. experimental results for the cantilever beam.

tions for instance), which is convenient from the signal processing point of view. Thus, we pose the identification task as a standard non-linear least squares minimization problem with the objective function expressed as follows:

$$F(\mu) = \left(\frac{\varepsilon_k^{\text{beam}} - \varepsilon_k^{\text{beamM}}}{\varepsilon_k^{\text{beamM}}} \right)^2 \quad (27)$$

The function (27) collects responses from selected k sensors placed in beam elements, where flexural strains are measured. Note that the measured strains, denoted by the superscript M, refer to horizontal beam elements (see Figs. 2 and 4), whereas modifications to the structure are introduced only in truss elements A, B, C of the contact layer. This is an important distinction, which implies building an extended influence matrix, D_{kj}^{ext} collecting not just the interrelations within the contact layer, but also the influence of the truss members on the connected beam members.

The axial strain in truss elements ε (of type A, B or C) depends non-linearly upon the modification coefficient μ (cf. (13)), which is further used as a variable in optimization. Natural constraints are imposed on the modification coefficient μ , which is non-negative by definition:

$$\mu_i \geq 0. \quad (28)$$

If delamination has been identified, the constraints (28) are active. Another formal constraint has to be imposed on μ , related to structural degradation:

$$\mu_i \leq 1. \quad (29)$$

Using (3) and (5) and building the extended influence matrix, the gradient of the objective function (27) with respect to the optimization variable μ is expressed as

$$\begin{aligned} \nabla F_i &= \frac{\partial F}{\partial \mu_i} = \frac{\partial F}{\partial \varepsilon_k^{\text{beam}}} \frac{\partial \varepsilon_k^{\text{beam}}}{\partial \varepsilon_j^0} \frac{\partial \varepsilon_j^0}{\partial \mu_i} \\ &= \frac{2}{(\varepsilon_k^{\text{beamM}})^2} (\varepsilon_k^{\text{beam}} - \varepsilon_k^{\text{beamM}}) D_{kj}^{\text{ext}} \frac{\partial \varepsilon_j^0}{\partial \mu_i}. \end{aligned} \quad (30)$$

The partial derivative $\frac{\partial \varepsilon_j^0}{\partial \mu_i}$ can be easily calculated by differentiating relation (24) or (26) with respect to μ :

$$\begin{bmatrix} \delta_{ij} - (1 - \mu_i^A) D_{ij}^A & -(1 - \mu_i^B) D_{ij}^B & -(1 - \mu_i^C) D_{ij}^C \\ -(1 - \mu_i^A) D_{ij}^A & \delta_{ij} - (1 - \mu_i^B) D_{ij}^B & -(1 - \mu_i^C) D_{ij}^C \\ -(1 - \mu_i^A) D_{ij}^A & -(1 - \mu_i^B) D_{ij}^B & \delta_{ij} - (1 - \mu_i^C) D_{ij}^C \end{bmatrix} \begin{bmatrix} \frac{\partial \varepsilon_j^{0A}}{\partial \mu_i} \\ \frac{\partial \varepsilon_j^{0B}}{\partial \mu_i} \\ \frac{\partial \varepsilon_j^{0C}}{\partial \mu_i} \end{bmatrix} = \begin{bmatrix} -\varepsilon_i^A \\ -\varepsilon_i^B \\ -\varepsilon_i^C \end{bmatrix} \quad (31)$$

Note that the left-hand side matrices in (26) and (31) are alike, which simplifies computations. Only the right-hand sides are different.

The optimization variable μ is updated according to the steepest descent method:

$$\mu_i^{(n+1)} = \mu_i^{(n)} - \alpha F^{(n)} \frac{\nabla F_i^{(n)}}{[\nabla F_i^{(n)}]^T \nabla F_i^{(n)}}. \quad (32)$$

Superscript (n) denotes values in current iteration and ($n + 1$) in subsequent iteration. The constant α varies in the range 0.1–0.3.

The algorithm solving the problem of identification of delamination processes the following stages:

A. Initial calculations

1. calculate response ε_i^L (contact layer, truss elements) and $\varepsilon_k^{\text{beamL}}$ (sensors, beam elements) of the intact structure subjected to external load, using a numerical model;
2. determine measured response $\varepsilon_k^{\text{beamM}}$ of the structure with introduced modifications using k sensors in experiment (alternatively, simulate the measured response numerically);

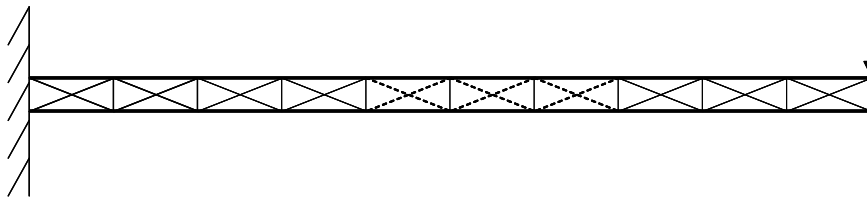


Fig. 17. Double-layer beam analyzed to identify delamination in statics.

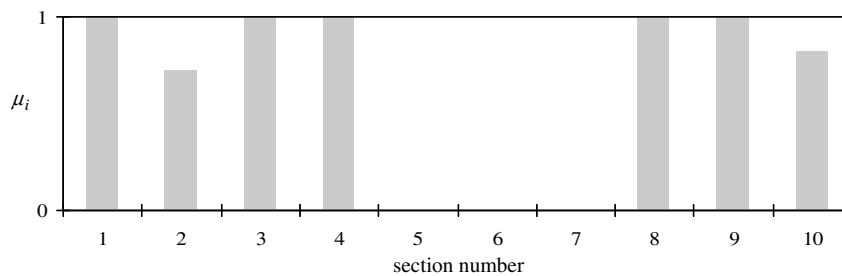


Fig. 18. Results of search for inner delamination – static load.

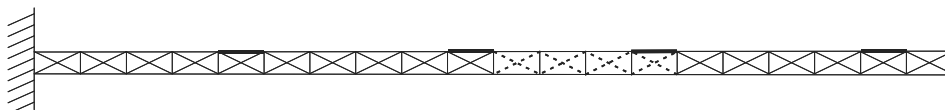


Fig. 19. Double-layer beam analyzed to identify inner delamination in dynamics.

3. compute the influence matrix D_{ij} for the contact layer and the extended influence matrix D_{kj}^{ext} including the truss-beam interactions;
4. set the initial value of optimization variable to unity $\mu_i = 1$, which implies $\varepsilon_i^0 = 0$, $\varepsilon_k = \varepsilon_k^{beam L}$.

B. Iterative calculations

1. store the current value F_{cur} of the objective function (27) as the former value F_{for} ;
2. solve the set (31) for partial derivatives $\frac{\partial \varepsilon_i^0}{\partial \mu_i}$;
3. calculate the gradient ∇F_i using (30);
4. determine next value of the variable $\mu_i^{(n+1)}$ using (32);
5. solve for distortions ε_i^0 , using (26);
6. update $\varepsilon_k^{beam L}$, using (5);
7. calculate the current value of the objective function F_{cur} ;

8. check the termination criterion – if $F_{cur}/F_{for} \leq 10^{-3}$ then STOP else go to B.1.

In dynamics, the stages are handled in each time step by the Newmark integration procedure.

4.2. Numerical off-line identification in statics and dynamics

For checking the effectiveness of the VDM-based identification algorithm, examples of double cantilever beams, presented in Sections 3.3 and 3.4, are used.

In statics, a cantilever beam, shown in Fig. 17, with the contact layer divided into 10 sections is analyzed (data as in section 3.3). The structure is subjected to a static force applied at the free end. The delamination zone extends over three sections 5–7. The beam is equipped with 20 sensors, located in each horizontal element of both the lower and upper beam. The results of

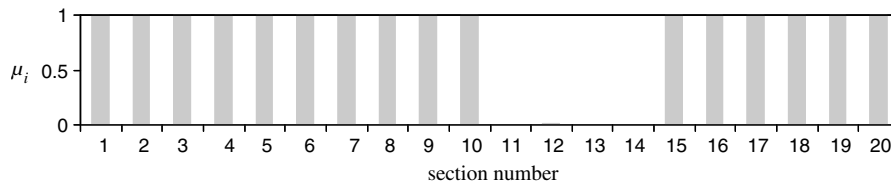


Fig. 20. Results of search for inner delamination – dynamic load.

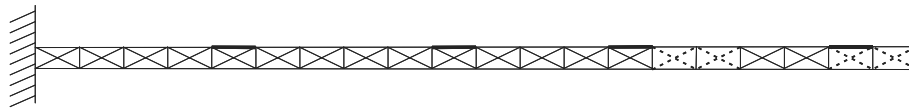


Fig. 21. Double-layer beam analyzed to identify inner and edge delamination in dynamics.

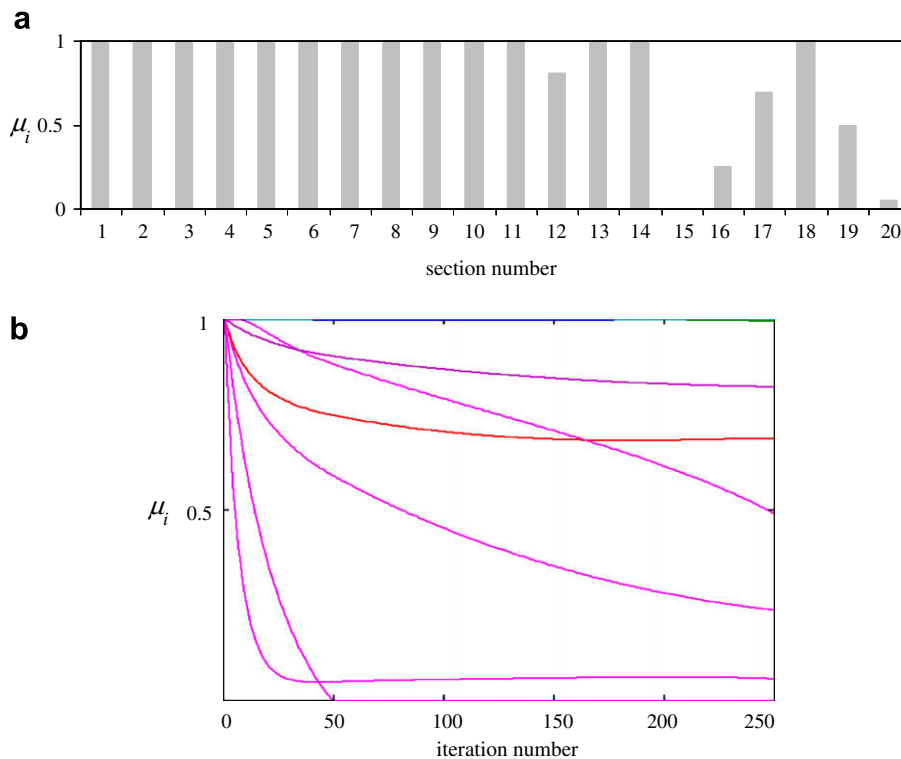


Fig. 22. (a) Results of search for inner and edge delamination – dynamic load; (b) variations of μ in 250 iterations.

identification, obtained after 200 optimization iterations, are shown in Fig. 18. The assumed zone of delamination has been detected correctly.

In dynamics, the contact layer, shown in Fig. 19, is divided into 20 sections (data as in section 3.4). An impulse sine load (cf. Fig. 15b) with a duration equal to the time period of the 4th eigenfrequency of the beam is applied as excitation at the free end. The delamination zone extends over four sections 11–14. Contrary to the static case, only four sensors mounted on the upper beam, marked by bold lines in Fig. 19, are considered in the identification process. The results reached after 300 iterations are presented in Fig. 20. The obtained accuracy is very good.

Another example in dynamics focuses on identification of two zones of delamination, depicted in Fig. 21, including the inner part and the edge of the cantilever beam. The damaged zone extends over sections 15–16 and 19–20 of the contact layer. This scenario

of delamination is harder to detect as can be seen in Fig. 22, however both zones of damage have been correctly located. The result can be improved with more sophisticated optimization.

4.3. Experimental verification of off-line identification in dynamics

Analogously to the experimental verification carried out for delamination modelling, described in section 3.5, similar measurements were collected to check the correctness of delamination identification. The same experimental stand was used. Delamination was applied by removing two screws tightening the two beams in the middle part of the structure, as shown in Fig. 14a. Thus the delamination extends over three sections of the contact layer modelled by VDM. The first stage was to tune numerical model to experimental response. It was achieved with the material data given in section 3.5. With the well-tuned model, identification algorithm was run and the results of delamination identification are shown in Fig. 23.

The agreement between the experiment and the simple numerical model with coarse discretization is very good. Due to the fact that the double beam was connected with screws, there is always some contact between layers in the vicinity of the screws. That is why the identified stiffness in the assumed delaminated sections close to the tightened screws does not drop to zero but just half the initial stiffness. In the middle section of assumed delamination, where both neighbouring screws are removed, the ideal zero value was detected.

4.4. Numerical on-line identification in dynamics

On-line identification of delamination is extremely important in some kinds of applications requiring “allow” or “not allow” decisions e.g. assessing structural health of a helicopter rotor in motion. Intuitively, it is likely that the problem will require more sensors, able to detect a defect quickly in real time.

The concept of on-line identification of delamination assumes a uniformly distributed net of sensors, acting in pairs, attached to the upper and lower surface of the double-layer beam structure, as shown in Fig. 24. Piezoelectric sensors measure voltage on upper and lower surface, which is proportional to flexural strain of the beam. Local delamination manifests itself in an apparent difference observed in responses of co-located (paired) sensors.

Numerical simulation was run to validate the idea. Fig. 25a depicts time signals captured by the sensors with delamination occurring in the midpoint of the analyzed period. The corresponding difference in response for the pairs of sensors is presented in Fig. 25b. The numerically assumed delamination extends over sections 13–15 and the difference in voltage clearly identifies this zone.

Experimental verification of this promising result will be pursued in the future.

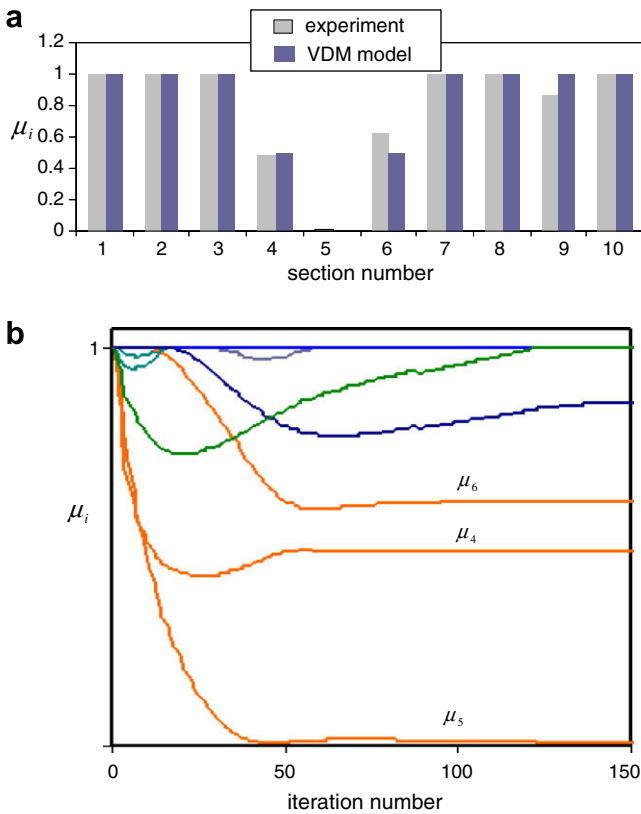


Fig. 23. (a) Numerical vs. experimental identification of delamination for the double-layer beam; (b) variations of μ in 150 iterations.

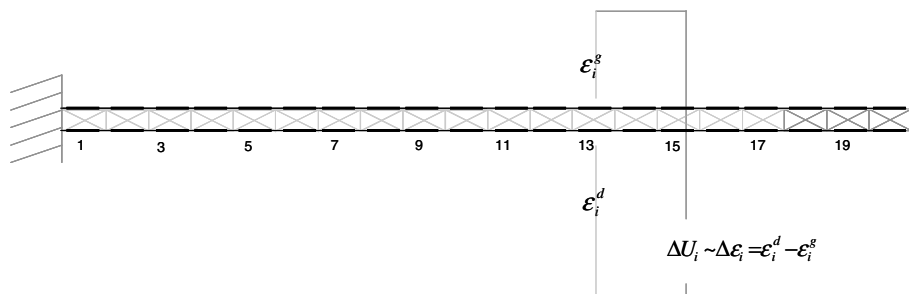


Fig. 24. The net of paired sensors able to detect delamination on-line.

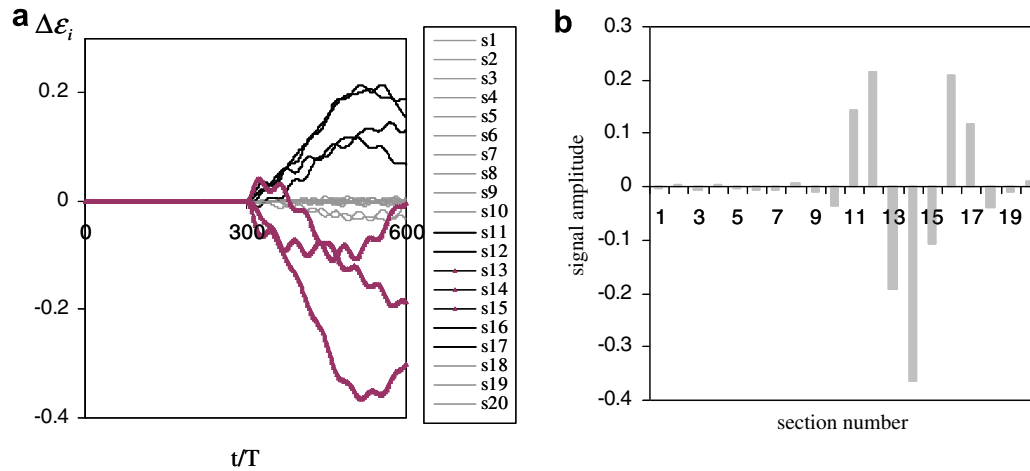


Fig. 25. (a) Time histories and (b) signal amplitudes for on-line identification of delamination.

5. Conclusions

The paper presents an idea of modelling and identification of delamination in a two-layer beam using the virtual distortion method. A novel concept of the contact layer, consisting of simple truss elements, connecting the two beam layers, has been proposed. The Bernoulli beam model and no friction between layers were the assumptions aiming at the reduction of numerical costs. However, the adopted model has turned out to follow the experiment faithfully for the problem of delamination modelling (see Fig. 16).

An approach for performing off-line identification by solving an analytically posed inverse problem has been proposed. With the adopted simplified model of the contact layer in between two beams, the identification has proceeded to expected solutions in reasonable computational time. The major difference between the static and dynamic approach is that we need many sensors in statics and only a few in dynamics. The reason is that the number of available data in statics is very limited while time histories of the monitored quantities in dynamics compensate the fact of mounting just a few sensors. However, the price to pay for the privilege of having lots of data in dynamics is a much more time-consuming numerical analysis. Good qualitative identification of two delamination zones, including the edge, has been achieved (see Fig. 22). Experimental verification of delamination identification in dynamics has also been successful, as evidenced in Fig. 23.

A proposition for on-line identification has been put forward. The problem has just been recognized at the numerical level. An experimental verification will be the subject of future research.

Acknowledgements

The authors gratefully appreciate the financial support from the projects 3T11F00930 and R0301502 granted by the State Committee for Scientific Research in Poland. The paper contains parts of the PhD thesis of the first author, supervised by the third author.

Parts of the paper have been incorporated into the book “Smart Technologies for Safety Engineering” edited by the third author, published by Wiley, April 2008.

References

- [1] Zhou Y, Tong L, Steven GP. Vibration-based model-dependent damage (delamination) identification and health monitoring for composite structures – a review. *J Sound Vib* 2000;230(2):357–78.
- [2] Meo M, Thieulot E. Delamination modelling in a double cantilever beam. *Compos Struct* 2005;71:429–34.
- [3] Iannucci L. Dynamic delamination modelling using interface elements. *Comput Struct* 2006;84:1029–48.
- [4] De Borst R, Remmers JCJ. Computational modelling of delamination. *Compos Sci Technol* 2006;66:713–22.
- [5] Kim H-Y, Hwang W. Effect of debonding on natural frequencies and frequency response functions of honeycomb sandwich beams. *Compos Struct* 2002;55:51–62.
- [6] Li HCH, Weis M, Herszberg I, Mouritz AP. Damage detection in a fibre reinforced composite beam using random decrement signatures. *Compos Struct* 2004;66:159–67.
- [7] Zak AJ. Non-linear vibration of a delaminated composite beam. *Key Eng Mater* 2005:607–14.
- [8] Bois C, Herzog P, Hochard C. Monitoring a delamination in a laminated composite beam using in-situ measurements and parametric identification. *J Sound Vib* 2007;299:786–805.
- [9] Ishak SI, Liu GR, Shang HM, Lim SP. Locating and sizing of delamination in composite laminates using computational and experimental methods. *Compos Part B: Eng* 2001;32:287–98.
- [10] Schnack E, Dimitrov S, Langhoff T-A. Computational identification on interface delaminations in layered composites based on surface measurements. *Arch Appl Mech* 2006;76:747–58.
- [11] Ramanujam N, Nakamura T, Urugo M. Identification of embedded interlaminar flaw using inverse analysis. *Int J Fract* 2005;132:153–73.
- [12] Holnicki-Szulc J, Gierlinski JT. Structural analysis, design and control by the virtual distortion method. Chichester, UK: J. Wiley & Sons; 1995.
- [13] Akgun MA, Garcelon JH, Haftka RT. Fast exact linear and non-linear structural reanalysis and the Sherman–Morrison–Woodbury formulas. *Int J Numer Methods Eng* 2001;50:1587–606.
- [14] Kolakowski P, Wiklo M, Holnicki-Szulc J. The virtual distortion method – a versatile reanalysis tool for structures and systems. *Struct Multidiscipl Optim*, in press, doi:10.1007/s00158-007-0158-7.
- [15] Ostachowicz W, Zak AJ. Vibration of a laminated beam with a delamination including contact effects. *Shock Vib* 2004;11:157–71.